

Infrared refractive indices of LaAlO₃, LaGaO₃, and NdGaO₃

Z. M. Zhang,* B. I. Choi,[†] and M. I. Flik

Department of Mechanical Engineering, Massachusetts Institute of Technology, Cambridge, Massachusetts 02139

A. C. Anderson

Lincoln Laboratory, Massachusetts Institute of Technology, Lexington, Massachusetts 02173

Received November 29, 1993; revised manuscript received May 19, 1994

We discuss the experimental and theoretical studies of the infrared optical constants of three perovskite materials: LaAlO₃, LaGaO₃, and NdGaO₃. These materials are commonly used as substrates for depositing high-temperature superconducting films. The transmittance and the reflectance are measured with a Fourier-transform infrared spectrometer. At frequencies from 1000 to 10 000 cm⁻¹, for which the substrates are transparent, the refractive index is extracted directly from the measured transmittance and reflectance. Kramers-Kronig relations are employed to yield the refractive index of these materials at frequencies from 100 to 1000 cm⁻¹. We also use a Lorentz phonon oscillator model to obtain the refractive index by fitting the measured data to the model function. The advantages and limitations of each method are discussed. The refractive index for the LaAlO₃ substrate is also obtained at 10 and 78 K with a cryogenic accessory. The results are compared with those reported by other research groups. This research provides information necessary for the quantitative study of the optical properties of thin superconducting films.

INTRODUCTION

Optical applications of high- T_c superconducting films require the knowledge of the infrared properties of the substrates, since the radiation penetration depth is often comparable with or larger than the film thickness.¹⁻³ To understand the radiative properties of the superconducting films, we must investigate the substrate refractive index. The optical properties of MgO and SrTiO₃, which were widely used as substrates for depositing high- T_c superconducting materials, were investigated previously by several research groups.⁴⁻⁷ Recently, high- T_c superconducting films were also grown on other substrates, such as LaAlO₃, LaGaO₃, and NdGaO₃, with good structural, electrical, and microwave properties.⁸⁻¹³ Few data exist for the optical properties of these materials.

In this paper the refractive indices of LaAlO₃, LaGaO₃, and NdGaO₃ are obtained from the measured reflectance and transmittance. In the spectral region between 1000 and 10 000 cm⁻¹, where the substrate is transparent, the substrate refractive index is extracted from reflectance and transmittance as was done by Choi *et al.*¹⁴ Kramers-Kronig analysis is applied to yield the refractive index in the spectral region between 100 and 1000 cm⁻¹ from the reflectance measurement. Dielectric functions are developed with the Lorentz-phonon-oscillators model for LaAlO₃, LaGaO₃, and NdGaO₃ at room temperature as well as for LaAlO₃ at 10 and 78 K. The error associated with the Kramers-Kronig analysis in the far-infrared region and that with the Lorentz model in the near-infrared region are discussed. The data and the phonon parameters reported by Calvani *et al.*¹⁵ and van der Marel *et al.*¹⁶ are compared with the results obtained from the present study.

EXPERIMENTS

A Biorad FTS-60A Fourier-transform infrared spectrometer is employed to measure the transmittance and the reflectance from 100 to 10 000 cm⁻¹ with various optical sources, beam splitters, and detectors.¹⁷ The effects of detector nonlinearity and nonequivalent responsivity on the measurement accuracy are reduced by appropriate throughput in the optical setup.^{18,19} Crystal samples with known transmittance, such as Si, Ge, CaF₂, MgO, and SrTiO₃, are used to calibrate the instrument. The uncertainty of the transmittance measurement is estimated to be within 1% at frequencies from 400 to 10 000 cm⁻¹ and 2% at frequencies from 100 to 400 cm⁻¹. The room-temperature reflectance is measured with an Au mirror as the reference and a 10° angle of incidence. The reflectance of Au is taken to be 0.99 at infrared frequencies from 100 to 10 000 cm⁻¹. The estimated uncertainty of the reflectance measurement is 3% at room temperature. A cryogenic accessory is employed for the investigation of optical properties at low temperatures. A detailed description of this apparatus was given by Zhang *et al.*¹⁷ The uncertainty of the reflectance measured at cryogenic temperatures is estimated to be 5% at frequencies from 450 to 2000 cm⁻¹ and 10% at frequencies from 100 to 450 cm⁻¹.

The substrates are grown by the Czochralski technique. Detailed descriptions of the crystal growth and the crystalline structure of these materials were given by O'Bryan *et al.*²⁰ The dimensions of the samples are nearly 12 mm × 12 mm × 0.5 mm. The crystalline wafers are cut nominally at the (100) orientation of the pseudocubic crystals. Note that at room temperature LaAlO₃ is rhombohedral, whereas LaGaO₃ and NdGaO₃

are orthorhombic. The samples of LaAlO₃ and LaGaO₃ are twinned because of phase transitions, which can be seen by the naked eye.

ANALYSIS

The sample thickness d is nearly 0.5 mm. The real part of the refractive index n of these substrates in the transparent region is close to 2. The free spectral range, $(2nd)^{-1}$, is $\sim 5 \text{ cm}^{-1}$. A resolution of 8 cm^{-1} is used in the Fourier-transform infrared measurements to remove the interference fringes. The resulting spectra are in the incoherent limit, and the interference effects need not be considered.²¹ The normal reflectance and transmittance of a substrate without consideration of interference are obtained by a ray-tracing method,²² that is,

$$R = \rho + \frac{\rho\tau^2(1-\rho)^2}{1-\tau^2\rho^2}, \quad (1)$$

$$T = \frac{\tau(1-\rho)^2}{1-\tau^2\rho^2}, \quad (2)$$

where τ is the transmittance along the path inside the substrate and ρ is the reflectivity of the air–substrate interface. They are related to the real and the imaginary parts of the refractive index, n and κ , and the thickness of the substrate, d , by

$$\tau = \exp\left(-\frac{4\pi\kappa d}{\lambda}\right), \quad (3)$$

$$\rho = \frac{(n-1)^2 + \kappa^2}{(n+1)^2 + \kappa^2}, \quad (4)$$

where λ is the wavelength in vacuum. The refractive index, reflectance, and transmittance are functions of frequency, which is omitted to simplify the expressions.

The refractive indices are extracted by three different methods. With the measured reflectance and transmittance, we obtain the substrate refractive indices by solving Eqs. (1)–(4), using the Newton–Raphson method.²³ This method is applicable only when the substrate is not opaque.

The Kramers–Kronig integrations relate the real and the imaginary parts of a causal response function.²⁴ In the case of reflectivity, the Fresnel reflection coefficient of the air–substrate interface is

$$\bar{r} = \rho^{1/2} \exp(i\phi) = \frac{n+i\kappa-1}{n+i\kappa+1}, \quad (5)$$

where the phase shift ϕ can be obtained if the reflectivity is known for all frequencies, i.e.,

$$\phi(\omega) = \frac{\omega}{\pi} \int_0^\infty d\omega' \frac{\ln \rho(\omega')}{\omega'^2 - \omega^2}, \quad (6)$$

where ω is the angular frequency. Extrapolations of the reflectivity to high and low frequencies are required, since the measured spectral range is between 100 and 10 000 cm^{-1} .

In the opaque region from 100 to 1000 cm^{-1} the measured reflectance R is equal to the reflectivity ρ . The dielectric constant at room temperature, ϵ_r , in the radio-frequency region is 23–26 for LaAlO₃, 25 of LaGaO₃, and

20–23 for NdGaO₃.^{8,11,13,25,26} The dielectric constant for these materials changes by less than 2% from 300 to 20 K.^{26,27} The reflectivity calculated from Eq. (5) with the refractive indices $n = \epsilon_r^{1/2}$ and $\kappa \sim 0$ is within 2% of the measured reflectivity at 100 cm^{-1} . Hence the reflectivity for frequencies below 100 cm^{-1} is assumed to be equal to that measured at 100 cm^{-1} .

The reflectivity ρ in the transparent region is calculated with the refractive index extracted from the measured transmittance and reflectance. The reflectivity at frequencies higher than 10 000 cm^{-1} is assumed to be constant and equal to the value at 10 000 cm^{-1} . The error in the phase shift caused by this extrapolation for $100 \text{ cm}^{-1} < \omega < 1000 \text{ cm}^{-1}$ is proportional to the frequency. The corrected phase shift is given by

$$\phi_c = \phi + \beta\omega. \quad (7)$$

We determine the constant β by comparing the phase shift near 1000 cm^{-1} calculated from Eq. (5), using the extracted refractive index, with that obtained from Eq. (6), as proposed by Choi *et al.*¹⁴

After the phase shift is obtained, the refractive index can be determined from

$$n = \frac{1-\rho}{1-2\rho^{1/2} \cos \phi_c + \rho}, \quad (8)$$

$$\kappa = \frac{2\rho^{1/2} \sin \phi_c}{1-2\rho^{1/2} \cos \phi_c + \rho}. \quad (9)$$

The dielectric function of a dielectric material in the infrared region, $\bar{\epsilon}$, can be modeled by use of the Lorentz phonon oscillators,²⁸ that is,

$$\bar{\epsilon}(\omega) = \bar{n}(\omega)^2 = \epsilon_\infty + \sum_{j=1}^N \frac{S_j \omega_j^2}{\omega_j^2 - \omega^2 - 2\gamma_j \omega}, \quad (10)$$

where $\bar{n} = n + i\kappa$ is the complex refractive index of the substrate, ϵ_∞ is the high-frequency dielectric constant, N is the number of phonons, and S_j , ω_j , and γ_j are the strength, center frequency, and width of the j th phonon, respectively. This model was used to model similar materials such as MgO and SrTiO₃.^{4–6}

As was discussed by Spitzer *et al.*,⁴ for the j th oscillator the product $n\kappa\omega$ has a maximum at its center frequency, ω_j . Therefore, the peaks of $n\kappa\omega$ calculated from the Kramers–Kronig analysis determine the center frequencies of phonon oscillators. Usually $\gamma_j \ll \omega_j$, and γ_j is equal to the full width at half-maximum of each $n\kappa$ peak. The strength of the resonance is determined by

$$S_j = 4n(\omega_j)\kappa(\omega_j) \frac{\gamma_j}{\omega_j}. \quad (11)$$

The value of ϵ_∞ is obtained from the near-infrared transmittance at 10 000 cm^{-1} , where the imaginary part of the refractive index is negligibly small. After the initial values are selected, the reflectance is calculated from Eq. (1). The values of S_j , ω_j , and γ_j are taken as initial values for the fitting. A multiple-parameter least-squares fitting program is employed.²³ It determines the best-fitting parameters by minimizing the quantity χ^2 , defined as

$$\chi^2 \equiv \sum_{m=1}^M \left[\frac{R_m - R_c(\lambda_m; \epsilon_\infty, \omega_1, S_1, \gamma_1 \dots \omega_N, S_N, \gamma_N)}{\sigma_m} \right]^2, \quad (12)$$

where R_m and σ_m are the measured reflectance and its standard deviation, M is the total number of data points, and R_c is the reflectance calculated from the Lorentz dielectric function.

At near-zero frequencies Eq. (10) reduces to

$$\bar{\epsilon}(0) = \epsilon_\infty + \sum_{j=1}^N S_j. \quad (13)$$

Equation (13) can be used to test the quality of the fit by comparison with the measured low-frequency dielectric constant.

RESULTS AND DISCUSSION

Figure 1 shows the measured reflectance of LaAlO_3 and that calculated from Eq. (10). The phonon oscillator parameters for all materials are listed in Table 1. The data obtained by Calvani *et al.*¹⁵ and van der Marel *et al.*¹⁶ are also shown for comparison. The reflectance calculated from Eq. (10) with the fitted parameters given in Table 1 is in good agreement with the measured reflectance. The reflectance obtained here is almost zero near 800 cm^{-1} , while that obtained by Calvani *et al.*¹⁵ is as large as 0.05. For similar materials, such as SrTiO_3 and BaTiO_3 , the reflectance also approaches zero near the absorption edge,⁴ where $n \sim 1$ and $\kappa \ll 1$. At 280 and 610 cm^{-1} the data of Calvani *et al.*¹⁵ are also consistently higher than the other data.

Figure 2 shows the refractive index obtained by three different methods. The refractive index calculated with the Lorentzian phonon parameters obtained by Calvani *et al.*¹⁵ is also shown for comparison. In the opaque region the refractive index obtained from the Kramers-Kronig relations is in reasonable agreement with that obtained from the Lorentz model. Owing to the uncertainty in the extrapolated far-infrared reflectivity, the imaginary part of the refractive index obtained from the Kramers-Kronig analysis has a large

Table 1. Fitted Parameters for the Lorentz Dielectric Function of all Three Substrates

Parameter	LaAlO_3 (300 K)	LaAlO_3 (10, 78 K)	LaGaO_3 (300 K)	NdGaO_3 (300 K)
ϵ_∞	4.0	4.0	4.1	4.1
$\omega_1 (\text{cm}^{-1})$	184	185	165	118
S_1	14.4	15.0	7.7	0.28
$\gamma_1 (\text{cm}^{-1})$	4.2	3.1	2.3	3.3
$\omega_2 (\text{cm}^{-1})$	428	427	275	174
S_2	4.1	4.2	6.7	5.5
$\gamma_2 (\text{cm}^{-1})$	2.7	1.6	8	5.4
$\omega_3 (\text{cm}^{-1})$	496	498	296	244
S_3	0.026	0.014	1.1	0.22
$\gamma_3 (\text{cm}^{-1})$	16	6.5	8	2.7
$\omega_4 (\text{cm}^{-1})$	652	594	308	255
S_4	0.27	0.005	2.0	0.13
$\gamma_4 (\text{cm}^{-1})$	23.5	7	10	4.9
$\omega_5 (\text{cm}^{-1})$	692	651	329	273
S_5	0.027	0.27	0.64	4.7
$\gamma_5 (\text{cm}^{-1})$	32	15	8	6.7
$\omega_6 (\text{cm}^{-1})$		674	353	290
S_6		0.014	0.029	1.2
$\gamma_6 (\text{cm}^{-1})$		49	4.1	6.7
$\omega_7 (\text{cm}^{-1})$			416	300
S_7				0.013
$\gamma_7 (\text{cm}^{-1})$			8	10.6
$\omega_8 (\text{cm}^{-1})$			510	321
S_8				0.038
$\gamma_8 (\text{cm}^{-1})$			23	22
$\omega_9 (\text{cm}^{-1})$			536	343
S_9				0.032
$\gamma_9 (\text{cm}^{-1})$			18	9.6
$\omega_{10} (\text{cm}^{-1})$			597	356
S_{10}				0.25
$\gamma_{10} (\text{cm}^{-1})$			30	6.4
$\omega_{11} (\text{cm}^{-1})$				424
S_{11}				0.062
$\gamma_{11} (\text{cm}^{-1})$				7.8
$\omega_{12} (\text{cm}^{-1})$				525
S_{12}				0.074
$\gamma_{12} (\text{cm}^{-1})$				32
$\omega_{13} (\text{cm}^{-1})$				591
S_{13}				0.17
$\gamma_{13} (\text{cm}^{-1})$				33

uncertainty at frequencies below 150 cm^{-1} . In the frequency region between 300 and 400 cm^{-1} the phase shift ϕ_c is less than 0.03 rad, which is comparable with $\beta\omega$ ($\beta = 9.2 \times 10^{-5} \text{ rad cm}$ for LaAlO_3). The uncertainty in the determination of the phase shift causes a large error in the κ value. Notice that the reflectance is a weak function of κ for $n > 2$ and $\kappa < 0.2$.

As is shown in Fig. 3, in the transparent region the transmittance calculated with the Lorentz model is much lower than the measured one. The Lorentz dielectric functions obtained by Spitzer *et al.*⁴ for SrTiO_3 and obtained by Jasperse *et al.*⁶ for MgO also underpredict the transmittance of these materials for $\omega > 1000 \text{ cm}^{-1}$. Therefore the simple Lorentz model overpredicts the imaginary part of the refractive index and is not applicable to the transparent region at frequencies higher than $\sim 1000 \text{ cm}^{-1}$. Adding more phonon oscillators in this region would increase κ . The transmittance calculated using the dielectric function obtained by Calvani *et al.*¹⁵ is always zero for a $446\text{-}\mu\text{m}$ film. As discussed by Barker,²⁹

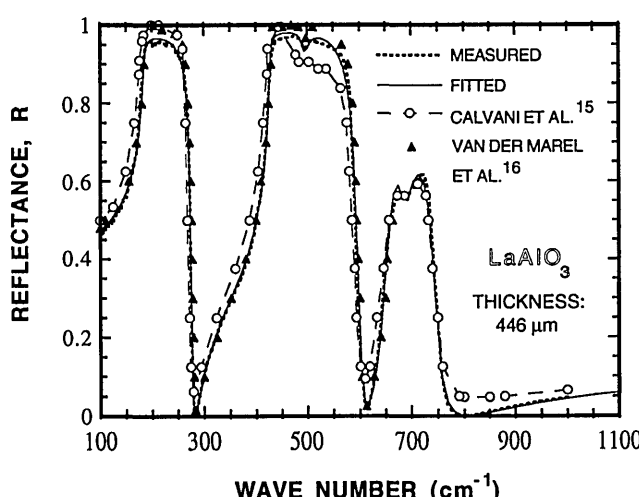


Fig. 1. Reflectance of LaAlO_3 at room temperature.

the damping coefficient γ_j is complex and frequency dependent. The absorptance of a crystal decreases more rapidly toward short wavelengths than that predicted by use of a frequency-independent damping coefficient. For $4\pi\kappa d/\lambda \ll 1$, the absorptance, $\alpha = 1 - T - R$, can be approximated by $4\pi\kappa d/\lambda$. With $d = 500 \mu\text{m}$ and $\lambda = 5 \mu\text{m}$, $\alpha \approx 10^3 \kappa$. The measured $T + R$ in the frequency region from 1500 to 10 000 cm^{-1} is greater than 0.99. Considering the measurement uncertainty, a conservative estimate would be that κ is less than 3×10^{-5} in this region.

As the frequency approaches zero, the dielectric function given by Eq. (10) approaches the sum of all S_j and the high-frequency constant ϵ_∞ . The value $\bar{\epsilon}(0) = 22.8$ obtained here is close to the dielectric constant of 23–26 for LaAlO_3 at low frequencies.^{13,25,26} The value calculated from the parameters obtained by Calvani *et al.*¹⁵ is 34, which is more than 40% higher than the measured value.

Figure 4 shows the measured and the calculated reflectance of LaAlO_3 at cryogenic temperatures. Little difference is observed between the reflectances at 10 and 78 K. The fitted reflectance is calculated from Eq. (10) for the parameters listed in Table 1. Near 700 cm^{-1} the reflectance increases by ~30% as the temperature is changed from room temperature to 78 K. A phonon oscillator at 595 cm^{-1} , which does not appear at room temperature, is observed at 10 and 78 K. The discrepancy

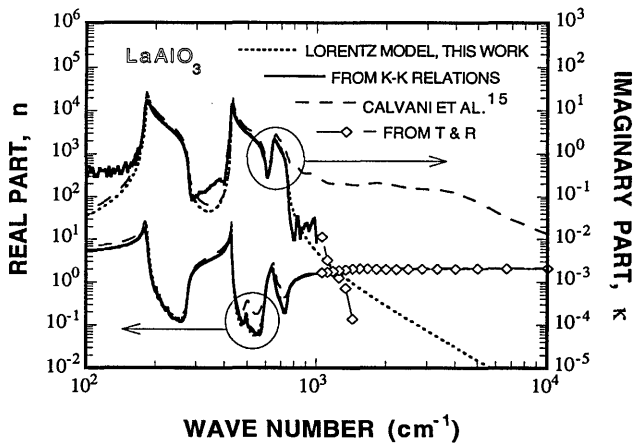


Fig. 2. Refractive index of LaAlO_3 at room temperature. K-K, Kramers-Kronig.

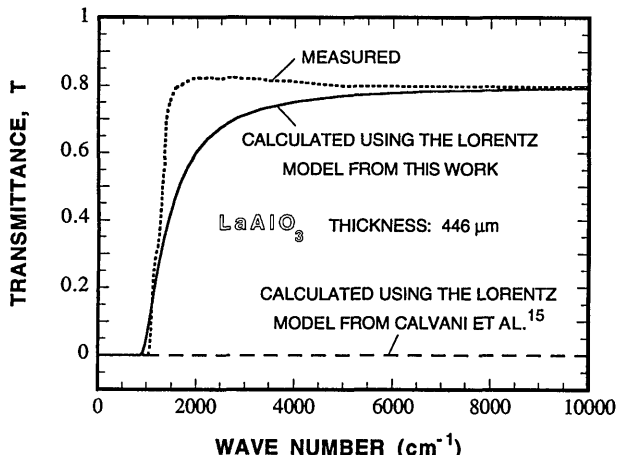


Fig. 3. Transmittance of LaAlO_3 at room temperature.

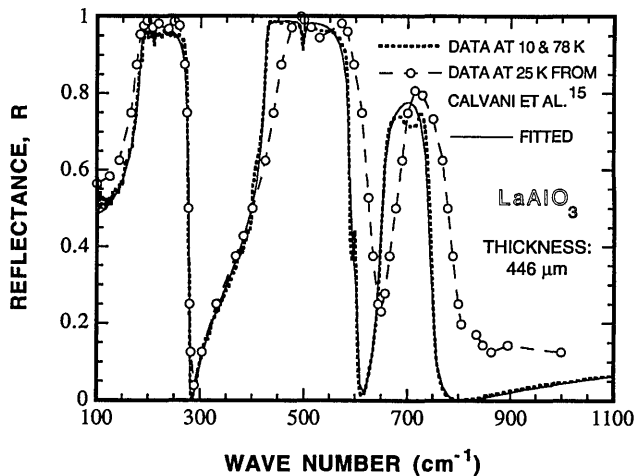


Fig. 4. Reflectance of LaAlO_3 at cryogenic temperatures.

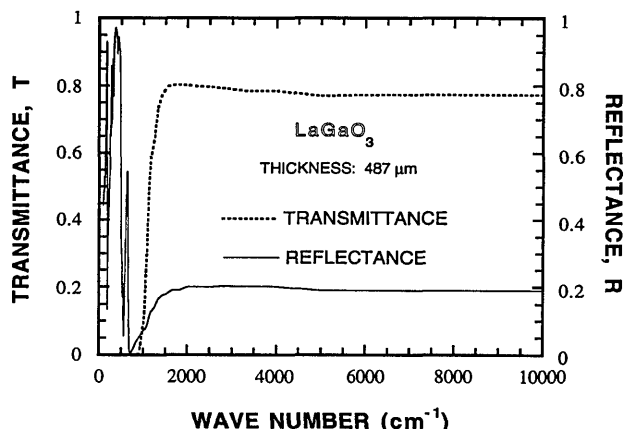


Fig. 5. Measured reflectance and transmittance of LaGaO_3 at room temperature.

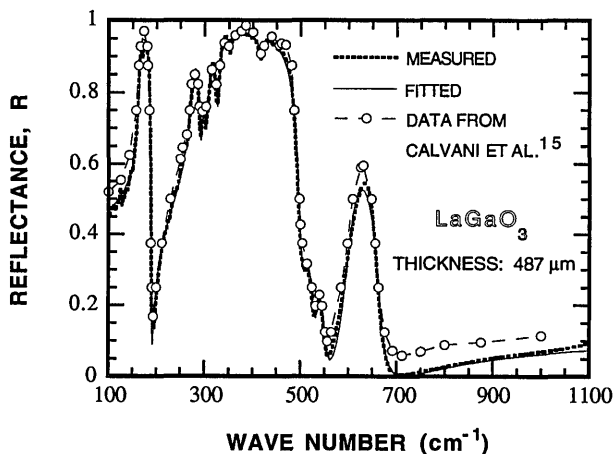


Fig. 6. Reflectance of LaGaO_3 at room temperature in the spectral region from 100 to 1100 cm^{-1} .

between the data obtained by this study and those from Calvani *et al.*¹⁵ is large in the midinfrared region. The data of Calvani *et al.*¹⁵ showed that the reflectance minimum near 610 cm^{-1} at room temperature was shifted to 650 cm^{-1} at 25 K, which cannot be explained physically. Microwave and radiowave experiments indicate that the dielectric constant of LaAlO_3 changes little from 300 to

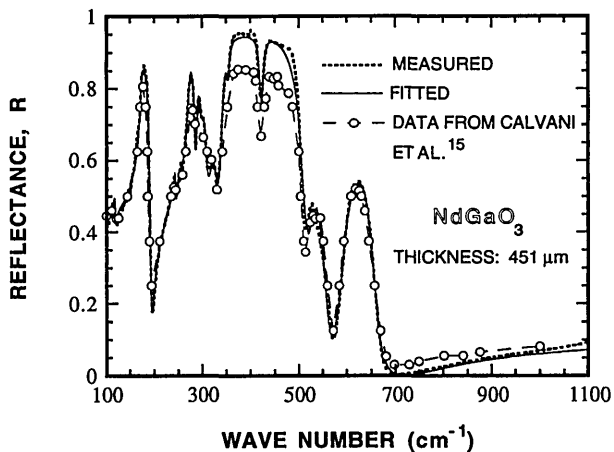


Fig. 7. Reflectance of NdGaO₃ at room temperature in the spectral region from 100 to 1100 cm⁻¹.

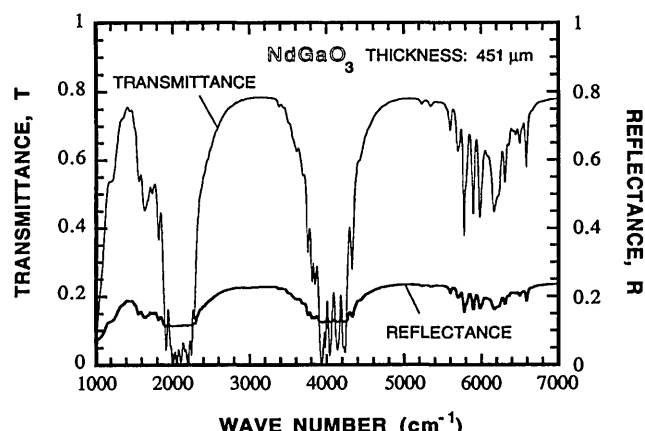


Fig. 8. Measured reflectance and transmittance of NdGaO₃ at room temperature in the spectral region from 1000 to 7000 cm⁻¹.

4 K. The low-frequency dielectric constant $\bar{\epsilon}(0)$, obtained from this study is 23.5, while that obtained by Calvani *et al.*¹⁵ is 43.9.

The reflectance and the transmittance of LaGaO₃ at room temperature are shown in Figs. 5 and 6. Figure 7 shows the measured and the calculated reflectance of NdGaO₃ at room temperature. There are more infrared active phonons in LaGaO₃ and NdGaO₃ than in LaAlO₃ and SrTiO₃. The transmittance of NdGaO₃ given in Fig. 8 shows many absorption peaks that are due to the transitions of Nd atoms. Similar features were observed by Calvani *et al.*¹⁵ Owing to the large uncertainty in the optical constants obtained by the Kramers-Kronig relations, the Lorentz dielectric function is recommended for LaGaO₃ and NdGaO₃ in the infrared region. In general the frequencies of the phonon modes agree well with those determined from infrared absorption spectra, Raman spectroscopy, and lattice-dynamics calculations.³⁰⁻³²

SUMMARY

Infrared optical constants are determined for three substrate materials from transmittance and reflectance measurements. In the absorbing region at frequencies from 100 to 1000 cm⁻¹ the refractive index obtained from the

Lorentz model is in good agreement with that determined from the Kramers-Kronig relations. In the transparent region at frequencies from 1000 to 10 000 cm⁻¹ the refractive index should be extracted from the measured reflectance and transmittance, since the Lorentz model overpredicts the κ value and underpredicts the transmittance. This investigation facilitates the study of the optical properties of high- T_c superconducting thin films, and it also helps in the optical design for applications that use superconducting film-substrate composites, such as high- T_c superconducting radiation detectors.

ACKNOWLEDGMENTS

Some of the samples were provided by M. P. Siegal and C. D. Brandle from AT&T Bell Laboratories and by A. J. Strauss from MIT Lincoln Laboratory. K. P. Steward of the NASA Goddard Space Flight Center is acknowledged for valuable comments. This research was sponsored by the C. S. Draper Laboratory, Cambridge, Massachusetts, contract DL-H-418480, and by the Defense Advanced Research Projects under the auspices of the Consortium for Superconducting Electronics, contract MDA972-90-C-0021.

*Present address, Radiometric Physics Division, National Institute of Standards and Technology, Gaithersburg, Maryland 20899.

[†]Present address, McKinsey & Company, Cleveland, Ohio 44114.

REFERENCES

1. M. I. Flik, Z. M. Zhang, K. E. Goodson, M. P. Siegal, and J. M. Phillips, "Electron scattering rate in epitaxial YBa₂Cu₃O₇ superconducting films," Phys. Rev. B **46**, 5606-5614 (1992).
2. Z. M. Zhang and M. I. Flik, "Predicted absorptance of YBa₂Cu₃O₇/YSZ/Si multilayer structures for infrared detectors," IEEE Trans. Appl. Supercond. **3**, 1604-1607 (1993).
3. C. G. Malone, Z. M. Zhang, M. I. Flik, and E. G. Cravalho, "Optimized design of far-infrared Fabry-Perot resonators fabricated from YBa₂Cu₃O₇," IEEE Trans. Appl. Supercond. **3**, 2852-2855 (1993).
4. W. G. Spitzer, R. C. Miller, D. A. Kleinman, and L. E. Howarth, "Far infrared dielectric dispersion in BaTiO₃, SrTiO₃, and TiO₂," Phys. Rev. **126**, 1710-1721 (1962).
5. A. S. Barker, Jr., and M. Tinkham, "Far-infrared ferroelectric vibration mode in SrTiO₃," Phys. Rev. **125**, 1527-1530 (1962).
6. J. R. Jasperse, A. Kahan, J. N. Plendl, and S. S. Mitra, "Temperature dependence of infrared dispersion in ionic crystals of LiF and MgO," Phys. Rev. **146**, 526-542 (1966).
7. J. C. Galerani and R. S. Katiyar, "The infrared reflectivity in SrTiO₃ and the antidistortive transition," Solid State Commun. **41**, 515-519 (1982).
8. R. L. Sandstrom, E. A. Giess, W. J. Gallagher, A. Segmüller, E. I. Cooper, M. F. Chisholm, A. Gupta, S. Shinde, and R. B. Laibowitz, "Lanthanum gallate substrates for epitaxial high-temperature superconducting thin films," Appl. Phys. Lett. **53**, 1874-1876 (1988).
9. D. W. Cooke, E. R. Gray, R. J. Houlton, B. Rusnak, E. A. Meyer, J. G. Beery, D. R. Brown, F. H. Garzon, I. D. Raistrick, A. D. Rollet, and R. Bolmaro, "Surface resistance of YBa₂Cu₃O₇ films on SrTiO₃ and LaGaO₃ substrates," Appl. Phys. Lett. **55**, 914-916 (1989).
10. G. Koren, A. Gupta, E. A. Giess, A. Segmüller, and R. B. Laibowitz, "Epitaxial films of YBa₂Cu₃O_{7-δ} on NdGaO₃, LaGaO₃, and SrTiO₃ substrates deposited by laser ablation," Appl. Phys. Lett. **54**, 1054-1056 (1989).

11. T. Scherer, R. Herwig, P. Marienhoff, M. Neuhaus, A. Vogt, and W. Jutzi, "Off-axis sputtered $\text{Y}_1\text{Ba}_2\text{Cu}_3\text{O}_{7-\delta}$ films on NdGaO_3 ," *Cryogenics* **31**, 975–978 (1991).
12. M. P. Siegal, J. M. Phillips, A. F. Hebard, R. B. van Dover, R. C. Farrow, T. H. Tiefel, and J. H. Marshall, "Off-axis sputtered $\text{Y}_1\text{Ba}_2\text{Cu}_3\text{O}_{7-\delta}$ films on NdGaO_3 ," *J. Appl. Phys.* **70**, 4982–4988 (1991).
13. J. M. Phillips, M. P. Siegal, R. B. van Dover, T. H. Tiefel, J. H. Marshall, C. D. Brandle, G. Berkstresser, A. J. Strauss, R. E. Fahey, S. Sengupta, A. Cassanho, and H. P. Janssen, "Comparison of $\text{Ba}_2\text{YCu}_3\text{O}_{7-\delta}$ thin films grown on various perovskite substrates by coevaporation," *J. Mater. Res.* **7**, 2650–2657 (1992).
14. B. I. Choi, Z. M. Zhang, M. I. Flik, and T. Siegrist, "Radiative properties of $\text{Y}-\text{Ba}-\text{Cu}-\text{O}$ films with variable oxygen content," *J. Heat Transfer* **114**, 958–964 (1992).
15. P. Calvani, M. Capizzi, F. Donato, P. Dore, S. Lupi, P. Maselli, and C. P. Varsamis, "Infrared optical properties of perovskite substrates for high- T_c superconducting films," *Physica C* **181**, 289–295 (1991).
16. D. van der Marel, H.-U. Habermeier, D. Heitmann, W. König, and A. Wittlin, "Infrared study of the superconducting phase transition in $\text{YBa}_2\text{Cu}_3\text{O}_{7-x}$," *Physica C* **176**, 1–18 (1991).
17. Z. M. Zhang, B. I. Choi, T. A. Le, M. I. Flik, M. P. Siegal, and J. M. Phillips, "Infrared refractive index of thin $\text{YBa}_2\text{Cu}_3\text{O}_7$ superconducting films," *J. Heat Transfer* **114**, 644–652 (1992).
18. D. B. Chase, "Nonlinear detector response in FT-IR," *Appl. Spectrosc.* **38**, 491–495 (1984).
19. M. I. Flik and Z. M. Zhang, "Influence of nonequivalent detector responsivity on FT-IR photometric accuracy," *J. Quant. Spectrosc. Radiat. Transfer* **47**, 293–303 (1992).
20. H. M. O'Bryan, P. K. Gallagher, G. W. Berkstresser, and C. D. Brandle, "Thermal analysis of rare earth gallates and aluminates," *J. Mater. Res.* **5**, 183–189 (1990).
21. Z. M. Zhang, "Optical properties of layered structures for partially coherent radiation," in *Heat Transfer '94, Proceedings of the Tenth International Heat Transfer Conference* (Taylor & Francis, Bristol, UK, 1994), Vol. 2, pp. 177–182.
22. R. Siegel and J. R. Howell, *Thermal Radiation Heat Transfer*, 3rd ed. (Hemisphere, Washington, D.C., 1992), Chap. 18.
23. W. H. Press, B. P. Flannery, S. A. Teukolsky, and W. T. Vetterling, *Numerical Recipes* (Cambridge U. Press, Cambridge, 1986), Chaps. 9 and 14.
24. F. Wooten, *Optical Properties of Solids* (Academic, New York, 1972), Chap. 6.
25. A. E. Lee, C. E. Platt, J. F. Burch, and R. W. Simon, "Epitaxially grown sputtered LaAlO_3 films," *Appl. Phys. Lett.* **57**, 2019–2021 (1990).
26. T. Konate, M. Sato, H. Asano, and S. Kubo, "Relative permittivity and dielectric loss tangent of substrate materials for high- T_c superconducting films," *J. Supercond.* **4**, 283–288 (1991).
27. G. A. Samara, "Low-temperature dielectric properties of candidate substrate for high-temperature superconductors: LaAlO_3 and $\text{ZrO}_2:9.5 \text{ mol. \% Y}_2\text{O}_3$," *J. Appl. Phys.* **68**, 4214–4219 (1990).
28. C. F. Bohren and D. R. Huffman, *Absorption and Scattering of Light by Small Particles* (Wiley, New York, 1983), Chaps. 2 and 9.
29. A. S. Barker, Jr., "Transverse and longitudinal optic mode study in MgF_2 and ZnF_2 ," *Phys. Rev. A* **136**, 1290–1295 (1964).
30. M. C. Saine, E. Husson, and H. Brusset, "Etude vibrationnelle d'aluminates et de gallates de terres rares—I. Aluminates de structure perovskite," *Spectrochim. Acta A* **37**, 985–990 (1981).
31. M. C. Saine, E. Husson, and H. Brusset, "Etude vibrationnelle d'aluminates et de gallates de terres rares—II. Gallates de structure perovskite," *Spectrochim. Acta A* **38**, 19–24 (1982).
32. M. Couzi and P. V. Huong, "Spectres infrarouges des perovskites de terres rares LZO_3 ($Z = \text{Al}, \text{Cr}, \text{Fe}, \text{Co}$)," *J. Chim. Phys.* **69**, 1339–1347 (1972).